Study of the $OH^- + CH_2F_2$ Reaction by Selected Ion Flow Tube Experiments and ab Initio Calculations

E. P. F. Lee,[†] J. M. Dyke,*[,†] and C. A. Mayhew[‡]

Department of Chemistry, The University, Southampton SO17 1BJ, U.K., and School of Physics and Astronomy, Birmingham University, Edgbaston, Birmingham B15 2TT, U.K.

Received: May 12, 1998; In Final Form: July 17, 1998

The reaction $OH^- + CH_2F_2 \rightarrow$ products has been investigated by both selected ion flow tube (SIFT) experiments and ab initio molecular calculations. The SIFT experiments showed that a bimolecular process, leading to two major anionic products, CHF_2^- (86%) and F^- (11%), and one minor anionic product, HF_2^- (3%), is in competition with a three-body association leading to $OH^-{\cdot}CH_2F_2$ (where values in parentheses are the relative values of the detected anionic products at 300 K). From a pressure dependence study, an upper limit of the bimolecular reaction rate coefficient at 300 K is determined to be $(2.4 \pm 1.4) \times 10^{-12}$ cm^3 molecule^{-1} s^{-1}. This shows a small negative temperature dependence, suggesting that the reaction proceeds via an ion-complex intermediate. These experimental results were rationalized using ab initio molecular orbital calculations. Stationary points on the reaction paths of the two main reaction channels were located at both the HF/6-31++G** and MP2/6-31++G** levels. The relative energies of the located stationary points were calculated at up to the CCSD(T)/6-311++G^{3df,2p}//MP2/6-31++G** level. The $CHF_2^- + H_2O$ channel was found to be endothermic by 7.5 kcal mol^{-1} and the $F^- + CH_2(OH)F$ channel was found to be exothermic by 20.4 kcal mol^{-1}. It was found that both reaction channels proceed via the reactant-like ion−molecule complex intermediate, $OH^-{\cdot}CH_2F_2$, in agreement with the conclusion drawn from the experimental negative temperature dependence of the overall rate coefficient. The fact that the product anion yields show that $[CHF_2^-] > [F^-]$, despite the fact that the $CHF_2^- + H_2O$ channel is endothermic whereas the $F^- + CH_2(OH)F$ channel is exothermic, has been rationalized using transition-state theory.

Introduction

Hydrofluorocarbons have received considerable attention in recent years, as they are considered as possible replacements for chlorofluorocarbons in industrial applications in order to reduce stratospheric ozone depletion (see, for example, ref 1 and references therein). In this connection, kinetic studies of relevant gas-phase reactions involving HFCs and the understanding of their reaction mechanisms would assist in understanding their fates in the atmosphere. We have recently published a detailed ab initio and selected ion flow tube (SIFT) study of the reaction $O^- + CH_2F_2 \rightarrow$ products.[2] This present study of the reaction $OH^- + CH_2F_2 \rightarrow$ products is an extension of this work and is part of a larger program of work to investigate anion−molecule reactions of importance in the upper atmosphere. These reactions are also of importance in instruments used for trace gas detection.[3] Related studies have been made by Grabowski and co-workers[4] on negative ion reactions with various chlorinated methanes using the flowing-afterglow and flowing-afterglow selected-ion flow tube methods.

In the case of the reaction $O^- + CH_2F_2 \rightarrow$ products, the reaction mechanisms are rather complex.[2] However, based on the results of the ab initio calculations, it was concluded that all the observed reaction channels proceed via a reactant-like anion−molecular complex, $O^-{\cdot}CH_2F_2$, followed by crossing onto the $OH{\cdot}CHF_2^-$ surface. Although CHF_2^- was not detected as an anionic product in the SIFT experiment, all the observed charged products (OH^-, CF_2^-, e^-) are derived from this surface. This study showed that the main experimental observations in the SIFT work could be satisfactorily accounted for, and it was suggested that, based on the results obtained, other anion−molecule reactions of the type $O^- + RH$ very probably proceed via an $OH{\cdot}R^-$ surface (i.e., via a proton transfer to the anionic species) even though R^- may not be an observed anionic product. In this connection, it would be of interest to investigate other anion−molecule reactions involving an anion other than O^- to see whether the proton abstraction step is still the initial step.

The hydroxyl anion, OH^-, has been chosen in the present study because of its significant role, which is similar to that of O^-, in the negative ion chemistry of the D region of the ionosphere.[5] Also, the proton affinities (PAs) of O^- and OH^-, −382.2 and −390.6 kcal mol^{-1}, respectively, as estimated from available experimental heats of formation ($\Delta H_{f,298}$) and electron affinities (EAs),[6] differ by only 8.4 kcal mol^{-1}. Therefore, it might be expected that the reactions of these two anionic species with difluoromethane would proceed by a similar mechanism. As will be discussed later, the reaction $OH^- + CH_2F_2 \rightarrow$ products is significantly slower than the $O^- + CH_2F_2$ reaction. Nevertheless, the main reaction channel does indeed proceed via a reactant-like intermediate, though the pathways after this intermediate are rather complex.

Experimental Section

As the SIFT apparatus and the experimental and data analysis methods utilized have been described in detail elsewhere,[7] only a brief description of the method used and experimental details relevant to this study will be presented here.

[†] The University.
[‡] Birmingham University.

10.1021/jp982224y CCC: $15.00
Published on Web 10/02/1998

OH^- anions were created in a high-pressure source using a 1:1 mixture of N_2O and CH_4 as the source gas. Dissociative attachment of electrons to N_2O produced O^- which then reacted rapidly with CH_4 to form OH^-. The reactions involved are

$$N_2O + e^- \rightarrow O^- + N_2 \quad (1)$$

$$O^- + CH_4 \rightarrow OH^- + CH_3 \quad (2)$$

The OH^- anions were mass-selected using a quadrupole mass filter, injected into a flow tube, and convected toward the reaction region by a fast helium flow ($\sim$150 Torr L s^{-1}) at a pressure of 0.4−0.7 Torr. To investigate the temperature dependence of the $OH^- + CH_2F_2$ reaction, the flow tube was first operated at 300 and then at 458 K. Commercially purchased CH_2F_2 was injected into the flow tube to give a known, controlled reactant neutral number density, which could be varied from 0 to $\sim 10^{13}$ cm^{-3}. The precursor and product anions were mass-analyzed using a second quadrupole mass spectrometer downstream of the inlet and were detected by a channeltron electron multiplier. Possible contamination of the injected ions by O^- was tested for using this mass spectrometer, and the ratio of O^- to OH^- was found to be less than 0.006. The decrease in the OH^- signal was monitored at different neutral flows to obtain rate coefficients. To ensure that the branching ratios for the primary product anions were not affected by secondary reactions, the product percentages were obtained by extrapolation to zero neutral reactant number density and were corrected for mass discrimination of the detection system. Values of product percentages are considered to be accurate to ±30% of the values quoted, although they are generally reproducible to better than this.

Computational Details

The general strategy used and the details of the calculations performed follow our recent work on the study of the reaction $O^- + CH_2F_2 \rightarrow$ products,[2] and therefore will only be summarized here. In brief, the reaction paths of the two main reaction channels observed experimentally (see next section) were studied at the HF/6-31++G** and MP2/6-31++G** levels by carrying out geometry optimization (to locate intermediates), transition-state (TS) search, and intrinsic reaction coordinate (IRC) calculations. Higher levels of theory have been employed than that used in the $O^- + CH_2F_2$ study[2] to evaluate reaction enthalpies because no experimental values for the electron affinity (EA) of CHF_2 and the heats of formation (ΔH_f) of CHF_2^- and $CH_2(OH)F$ are available (see later text and ref 8). As well as the HF/6-31++G** and MP2/6-31++G** levels, the G1, G2 (MP2), and G2 methods[9−11] were employed to obtain the reaction enthalpies for the two main observed reaction channels. In addition, the relative energies of all the stationary points located on the reaction paths were evaluated at the CCSD(T)/6-311++$G^{3df,2p}$//MP2/6-31++G** level, the highest level of calculation performed in this work. Full counterpoise (CP) correction for basis set superposition error[12] was employed at this level to obtain the CP-corrected relative electronic energy difference between the TS obtained and the reactants (see the next section).

Because all the reactants and products of interest have closed-shell singlet ground states, it is essentially the closed-shell singlet hypersurface which is of interest. Nevertheless, all calculations have employed unrestricted-spin wave functions. This is in case some open-shell singlet contributions might be important on parts of the reaction path due to bond breaking. However, the computed $\langle S^2 \rangle$ values were found to be zero in all cases. CASSCF (4, 4), CASSCF (4, 6), and CASSCF (6, 6) calculations were also carried out with the 6-31++G** basis set on the reactant-like intermediate and the TS obtained (see later text) at the MP2/6-31++G** optimized geometries. All CASSCF calculations gave only one major configuration, which was the expected closed-shell configuration, suggesting that nondynamic electron correlation is not important for the reactant-like intermediate and TS obtained (as has been found in the $O^- + CH_2F_2$ study, see ref 2). All calculations were carried out using the Gaussian 94[13] suite of programs at the Rutherford Laboratory (RL, EPSRC) on the Dec 8400 computer.

Results and Discussion

SIFT Results. When association occurs, the kinetic results are interpreted in terms of the kinetic scheme

$$A + OH^- \xrightarrow{k_r} \text{products} \quad (3)$$

$$A + OH^- \underset{k_{-a}}{\overset{k_a}{\rightleftharpoons}} (A{\cdot}OH^-)^* \quad (4)$$

$$(A{\cdot}OH^-)^* + He \xrightarrow{k_s} A{\cdot}OH^- + He \quad (5)$$

which allows for competition between bimolecular reaction 3 and association reactions 4 and 5. For this scheme, the effective bimolecular rate coefficient is pressure dependent:

$$k_2^{\text{eff}} = k_r + \frac{k_s k_a [He]}{k_{-a} + k_s [He]} \quad (6)$$

As an association product was identified for the reaction of OH^- with CH_2F_2, the pressure dependence of k_2^{eff} was examined by running the SIFT at helium pressures between 0.4 and 0.7 Torr. It was found that, for the two temperatures used in this study, the association reactions were in the "unsaturated" region, where k_2^{eff} increases linearly with helium pressure, i.e.

$$k_2^{\text{eff}} = k_r + \frac{k_s k_a [He]}{k_{-a}} \quad (7)$$

By fitting the pressure dependence of k_2^{eff} to eq 7, the bimolecular rate coefficient k_r was extracted from the data. These results are presented in Table 1 for the two temperatures used in this study. This approach has been used previously; see, for example, ref 14. It should be noted that, because of a small impurity in the CH_2F_2 sample, which resulted in a Cl^- signal (masses 35 and 37 amu were seen in the mass spectra) with an intensity comparable to HF_2^-, the rate coefficients obtained should be taken as upper limits.

The observed anionic product distributions are also given in Table 1 together with the corresponding probable neutral products. For the major reaction channel, production of CHF_2^- (86% at 300 K), the neutral product can safely be assumed to be water. However, for the remaining minor channels, because of unavailability of the experimental heats of formation for some of the species listed in Table 1, it was not possible to establish the enthalpies of the reactions which would produce the suggested neutral products. Ab initio calculations were therefore required to clarify this situation (see Computational Details and ab Initio Results sections). Since the HF_2^- branching percentage is small and because we cannot rule out that the weak signal observed at $m/z = 39$ amu is a result of the reaction of OH^- with an impurity in the CH_2F_2 sample, the HF_2^- product was

TABLE 1: Summary of SIFT Experimental Results for the Reaction $OH^- + CH_2F_2 \rightarrow$ Products

temp (K)	detected products (%)	probable neutrals	two-body rate coefficient, k_r (cm^3 molecules$^{-1}s^{-1}$)
300	CHF_2^-(86) F^- (11) HF_2^- (3)	H_2O $CH_2F(OH)$, CH_3OF CH_2O	$(2.4 \pm 1.4) \times 10^{-12}$
458	CHF_2^-(92) F^- (7) HF_2^- (1)	H_2O $CH_2F(OH)$, CH_3OF CH_2O	$(1.6 \pm 0.8) \times 10^{-12}$

TABLE 2: Computed ΔE_e Values and Reaction Enthalpies (ΔH) at Various Levels of Theory for the Reaction $OH^- + CH_2F_2 \rightarrow H_2O + CHF_2^-$

method	ΔE_e (kcal mol^{-1})	ΔH^{0K} (kcal mol^{-1})	ΔH^{298K} (kcal mol^{-1})
HF/6-31++G**[a]	7.19	5.00	5.39
MP2/6-31++G**[b]	10.75	8.49	8.70
G1	11.05	8.98	8.76
G2 (MP2)	10.44	8.37	9.37
G2	10.78	8.71	9.10
CCSD(T)/6-311++G(3df,2p)[c]	9.28	7.02	7.53

[a] At HF/6-31++G** optimized geometries and with unscaled HF/6-31++G** frequencies for ZPE correction. [b] At MP2/6-31++G** optimized geometries and with unscaled MP2/6-31++G** frequencies for ZPE correction. [c] At MP2/6-31++G** optimized geometries and with unscaled MP2/6-31++G** frequencies for ZPE correction.

TABLE 3: Computed ΔE_e Values and Reaction Enthalpies (ΔH) at Various Levels of Theory for the Reaction $OH^- + CH_2F_2 \rightarrow CH_2(OH)\,F + F^-$

method	ΔE_e (kcal mol^{-1})	ΔH^{0K} (kcal mol^{-1})	ΔH^{298K} (kcal mol^{-1})
HF/6-31++G**[a]	−26.40	−23.90	−24.28
MP2/6-31++G**[b]	−26.79	−24.71	−24.81
G1	−23.12	−20.56	−20.92
G2 (MP2)	−21.73	−19.17	−19.52
G2	−22.54	−19.98	−20.34
CCSD(T)/6-311++G(3df,2p)[c]	−22.35	−20.27	−20.37

[a] At HF/6-31++G** optimized geometries and with unscaled HF/6-31++G** frequencies for ZPE correction. [b] At MP2/6-31++G** optimized geometries and with unscaled MP2/6-31++G** frequencies for ZPE correction. [c] At MP2/6-31++G** optimized geometries and with unscaled MP2/6-31++G** frequencies for ZPE correction.

not considered in the ab initio calculations. It should be noted that $[F^-]$ and $[HF_2^-]$ increased with increasing $[CH_2F_2]$, suggesting possible contributions from secondary reactions. In addition, the small negative temperature dependence for the two-body rate coefficient suggests that the bimolecular reaction probably proceeds via an intermediate,[15] which in the environment of the SIFT can be collisionally stabilized.

Ab Initio Results. **Reaction Enthalpy of Reaction 8.** The computed electronic energy differences (ΔE_e) and reaction enthalpies (ΔH) at various levels of theory are summarized in Tables 2 and 3, respectively, for the two main reaction channels

$$OH^- + CH_2F_2 \rightarrow H_2O + CHF_2^- \quad (8)$$

$$OH^- + CH_2F_2 \rightarrow CH_2(OH)F + F^- \quad (9)$$

For reaction 8, although the computed ΔH value at the Hartree−Fock (HF) level differs significantly from the ΔH values derived using methods which allow for electron correlation (see Table 2), it is conclusive from the results of this work that reaction 8 is endothermic. Excluding the CCSD(T) reaction enthalpy, the spread of ΔH values calculated at the correlated level is only 0.6 kcal mol^{-1}. The CCSD(T) value, which is expected to be the most reliable, is, however, lower than the G2 value. This suggests that higher order correlation is important and that corrections for the inadequacy of the basis set are not additive for this system, as assumed in the G1/G2 approach.

Experimental heats of formation are available for OH^-, H_2O, and CH_2F_2 (−34.4, −57.8, and −107.4 kcal mol^{-1} at 298 K respectively[6,16]), but not for CHF_2^-. Although the heat of formation of CHF_2 is available (−57.1, −58.6, and −59.2 kcal mol^{-1} from refs,17, 18, and 19, respectively), the reliability of the only available experimental EA of CHF_2, (1.3 ± 0.3) eV,[20] has been questioned[8] from a comparison of the MP4/6-311++$G^{2df,p}$//HF-6-31++G** derived values of 0.77 (from an isodesmic reaction) and 0.79 eV (from a isogyric reaction).[8] (An alternative value of 1.21 eV has been determined,[21] but it probably has a larger error than the value of ref 20). It was noted in ref 8 that the experimental EA of CHF_2 of 1.3 eV was obtained from potentially unreliable bracketing experiments. If this value is used to evaluate the ΔH of reaction 8, a value of −3.8 kcal mol^{-1} is obtained. On the other hand, using the MP4//HF value of 0.79 eV from ref 8, a value of +8.0 kcal mol^{-1} is obtained. The computed results of this present work clearly support the conclusions of ref 8, though the EA of CHF_2 has not been calculated directly by ab initio calculations. Nevertheless, using the best ab initio ΔH calculated for reaction 8 and the available experimental heats of formation (at 298 K) for OH^-, CH_2F_2, and H_2O, $\Delta H_{f,298}$ of CHF_2^- is deduced as −77.8 kcal mol^{-1}. From the available experimental heats of formation of CHF_2 (−57.1, −58.6, and −59.2 kcal mol^{-1} from refs 17, 18, and 19, respectively), values of 0.90, 0.83, and 0.81 eV can be obtained for the EA of CHF_2. The recommended value for the EA of CHF_2 is therefore (0.85 ± 0.05) eV.

Reaction Enthalpy of Reaction 9. For reaction 9, geometry optimization and vibrational frequency calculations were carried out also for CH_3OF, an isomer of $CH_2(OH)F$, at the MP2/6-31++G** level, because the experimental heat of formation of CH_3OF is not available. The minimum-energy geometry obtained for a CH_3OF structure, which has all real vibrational frequencies, has a C_s staggered structure and is calculated to be 83.9 kcal mol^{-1} higher in energy than $CH_2(OH)F$. Therefore, it is unlikely that CH_3OF would be the neutral product of reaction 9, as the reaction producing it would be endothermic by ca. 60 kcal mol^{-1} at the MP2/6-31++G** level.

From Table 3, the computed reaction enthalpies for reaction 9 are almost identical at the HF and MP2 levels, suggesting that the HF and MP2 hypersurfaces for this channel are similar. The reaction path study indeed showed that this was the case (see the next subsection). However, it is also clear from Table 3 that higher order electron correlation is important for reliable reaction energies. In contrast to reaction 8, the G1/G2 methods gave reaction enthalpies for reaction 9 which are almost identical to that obtained by the CCSD(T) method but are ca. 4 kcal mol^{-1} more positive than the HF and MP2 values. Although an experimental ΔH_f of $CH_2(OH)F$ is not available, it can be concluded from the present ab initio calculations that reaction

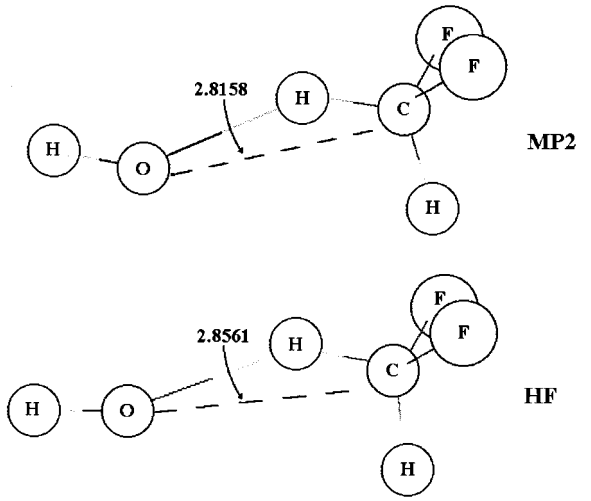

Figure 1. The minimum-energy structure of the reactant-like intermediate, $OH^-\cdot CH_2F_2$, computed at the HF/6-31++G** and MP2/6-31++G** levels for the $HO^- + CH_2F_2$ reaction. The O−C bond distance is given in angstroms in each case.

9 is exothermic by ca. 20 kcal mol^{-1}. Combining available experimental heats of formation (at 298 K) and the best ab initio ΔH for reaction 9 (the CCSD(T)/6-311++G^{3df,2p} value), the ΔH_f of $CH_2(OH)F$ can be deduced to be −103.0 kcal mol^{-1}.

From the ab initio results discussed above, reaction 8 should be slightly endothermic, while reaction 9 should be fairly exothermic. Clearly, the computed reaction enthalpies of these two reaction channels cannot account for the observed product distributions from the SIFT measurements, which clearly show that reaction 8 is the major channel while reaction 9 is the minor channel. To understand the SIFT results, the reaction hypersurface between the reactants and the products has to be investigated.

Reaction Path of Reaction 8: Production of CHF_2^-. *(a) HF/6-31++G** Calculations.* The reactant-like intermediate obtained, $OH^-\cdot CH_2F_2$, has C_s symmetry and is shown in Figure 1. It was computed to be 19.4 kcal mol^{-1} below the reactants (18.4 kcal mol^{-1} including the zero-point energy (ZPE) correction). Optimization with a C_s symmetry constraint for the product-like intermediate, $H_2O\cdot CHF_2^-$, however, led to a first-order saddle point with an a″ mode having an imaginary frequency of 34.7i cm^{-1}. On relaxing the symmetry constraint to C_1, a true minimum was obtained, but this is only 0.02 kcal mol^{-1} lower in energy than the C_s saddle point; the lowest computed frequency for this C_1 minimum was 39.4 cm^{-1}. These results suggest that the HF/6-31++G** surface in this region is extremely flat. A TS search gave a late transition-state structure, resembling the C_s product-like structure but with a shorter CO distance (2.614 Å instead of 2.940 Å as in the product-like intermediate). This TS is 12.7 (8.9) and 3.3 (0.3) kcal mol^{-1} above the reactant-like and product-like intermediates, respectively, and 13.9 (14.5) and 6.7 (9.5) kcal mol^{-1} below the separate products and reactants, respectively (where the values quoted in parentheses are the enthalpy differences which include ZPE correction). However, IRC path calculations gave the same reactant-like intermediate in both the forward and backward directions. This is almost certainly because, while the TS has a C_s symmetry, the product-like intermediate has a lower symmetry, C_1. In view of the results obtained for the IRC search and the product-like intermediate, the HF/6-31++G** level seems inadequate to describe the hypersurface of reaction 8. This was shown to be indeed the case as the more reliable MP2 results were found to differ significantly from the HF results; the MP2 results will be discussed in the next section.

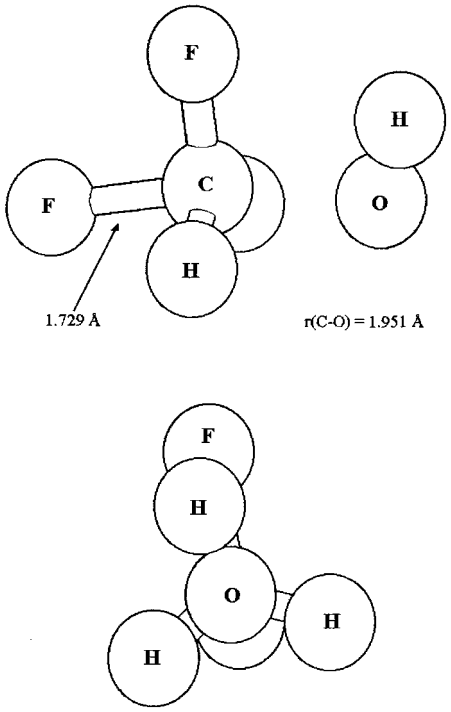

Figure 2. The TS obtained for the $OH^- + CH_2F_2 \rightarrow F^- + CH_2(OH)F$ reaction. HF/6-31++G** and MP2/6-31++G** calculations gave very similar structures for this TS. The C_1 structure shown in this figure with long C−F and C−O bond lengths (1.729 and 1.951 Å, respectively) was obtained at the MP2/6-31++G** level. This diagram shows two views of the transition-state structure, one at right-angles to the other.

*(b) MP2/6-31++G** Calculations.* With this basis set, a reactant-like intermediate similar to that obtained at the HF/6-31++G** level has been located (Figure 1). However, both optimization of the product-like intermediate and a TS search led to the conclusion that the reaction proceeded from the reactant-like intermediate directly to the separate products.[22] This was so with various starting geometries on the reaction hypersurface. In summary, the MP2/6-31++G** calculations gave only a valley, which is the reactant-like intermediate, $OH^-\cdot CH_2F_2$, between the reactants and the products. At the MP2/6-31++G** level, the reactant-like intermediate is 21.1 (18.6) and 31.8 (27.1) kcal mol^{-1} below the reactants and products (see also Table 4) where, as before, the values in parentheses are the enthalpies which include ZPEs. There is no barrier on the reaction surface. The reaction path rises smoothly to the separate products from the reactant-like intermediate. In this connection, the endothermicity of the reaction (ΔH at the CCSD(T)/6-311++G^{3df,2p}//MP2/6-31++G** level; see Table 2) may be taken as a lower limit of the energy barrier ($\Delta H^‡$ for the TS) for reaction 8 in a simplistic treatment. Taking the entropy change of the reaction (ΔS_{298K} = 5.8 cal mol^{-1} K^{-1} at the MP2/6-31++G** level) as $\Delta S^‡$ to the TS, $\Delta G^‡$ and the rate coefficient can be calculated as 5.8 kcal mol^{-1} and 5.9 × 10^{-13} cm^3 $molecule^{-1}$ s^{-1} at 298 K, respectively, employing conventional TS theory.[23]

Reaction Path of Reaction 9: Production of F^-. The HF/6-31++G** and MP2/6-31++G** results are qualitatively similar for the reaction hypersurface of reaction 9. The located TS is shown in Figure 2. It has a C_1 structure with long CF and CO bond lengths (1.729 and 1.951 Å, respectively, at the MP2/6-31++G** level), which suggests an S_N2 mechanism.

TABLE 4: Computed Relative Energies, ΔE_e (in kcal/mol), of the Stationary Points for the Reaction Channel, $OH^- + CH_2F_2 \rightarrow F^- + CH_2(OH)F$, at Various Levels of Calculations

ΔE_e (kcal/mol)	HF/ 6-31++G**	MP2/ 6-31++G**	CCSD(T)/ 6-311++G(3df,2p)[a]
$OH^- + CH_2F_2$	0.0	0.0	0.0
$OH^-\cdot CH_2F_2$	−19.4	−21.1	−20.1
TS	+5.8	−4.2[b]	−2.3[c]
$F^- + CH_2(OH)F$	−26.4	−26.8	−22.4

[a] At the MP2/6-31++G** optimized geometries. [b] $\Delta S^{\ddagger}$ at the MP2-6-31++G** level is −27.6 cal mol^{-1} K^{-1} at 298 K (see text). [c] The CP-corrected $\Delta E_e^{\ddagger}$ is +1.1 kcal/mol; the corresponding $\Delta H^{\ddagger,298K}$ is +0.9 kcal/mol (employing unscaled MP2/6-31++G** frequencies; see text).

Subsequent IRC path calculations at both the HF/6-31++G** and MP2/6-31++G** levels connected the TS with the reactant-like intermediate and the separate products (without going through a product-like intermediate).

Further geometry optimizations were carried out in search of the product-like intermediate. At the HF/6-31++G** level, a minimum with all real frequencies (the lowest being 87 cm^{-1}) was obtained. It has essentially a $F^-(HO)CH_2F$ structure (C_1 symmetry), with the F^- group bonded to the hydroxyl hydrogen. This was despite an initial geometry where the F^- group was on the opposite side of the hydroxyl group, adjacent to the two methylene hydrogen atoms. The F- - -H and OH bond lengths are 1.289 and 1.064 Å, respectively. This structure has a relative energy (ΔE_e) of −61.7 kcal mol^{-1} with respect to the separate reactants at the HF/6-31++G** level. At the MP2 level, however, a product-like intermediate could not be located. Instead, geometry optimization of over thirty points on the hypersurface led to a structure (which is not a stationary point) which is essentially $CH_2FO^-\cdot HF$ with HF and O- - -H bond lengths of 1.138 and 1.214 Å, respectively. That is, F^- has abstracted the proton from the hydroxyl group. Further optimization to a stationary point has not been carried out, as CH_2FO^- has not been detected experimentally. Nevertheless, it seems clear that at the MP2/6-31++G** level the anionic complex, $F^-\cdot CH_2(OH)F$, does not form as a stable intermediate as it proceeds to the $CH_2FO^-\cdot HF$ surface without a barrier. Since the IRC path discussed above has already shown that reaction 9 proceeds from the TS directly to the separate products, both the anion−molecule complex, $F^-\cdot CH_2(OH)F$ and the $CH_2FO^-\cdot HF$ surface are probably of little significance in determining the kinetics and dynamics of reaction 9.

The relative energies of the located stationary points at different levels of calculation are shown in Table 4. Relative to the reagents, a reactant-like intermediate $OH^-\cdot CH_2F_2$ is located at −20.1 kcal mol^{-1}, and later in the reaction a TS is located at −2.3 kcal mol^{-1}. This converts to the products $F^- + CH_2(OH)F$ at −22.4 kcal mol^{-1} with no product-like intermediate. If the enthalpy (ΔH) and the entropy differences (ΔS) between the TS and the separate reactants (see Table 4 and its footnotes) are taken to be $\Delta H^{\ddagger}$ and $\Delta S^{\ddagger}$, respectively, then $\Delta G^{\ddagger}$ and the rate coefficient of reaction 9 can be calculated using conventional TS theory[23] as 9.2 kcal mol^{-1} and 2.0×10^{-15} cm^3 $molecule^{-1}$ s^{-1}, respectively, at 298 K (using CCSD-(T)/6-311++$G^{3df,2p}$ values; see Table 4).

Comparison between Theory and Experiment. Comparing the calculated rate constants of reactions 8 and 9 obtained here (5.9×10^{-13} and 2.0×10^{-15} cm^3 $molecule^{-1}$ s^{-1} at 300 K) with the experimentally derived values, there is reasonably good qualitative agreement between the measured upper limit of the two-body rate constant k_r and the calculated value of eq 8. Also, the calculated rate constants show that $k_8 > k_9$, supporting the experimental result that $[CHF_2^-] > [F^-]$. With the standard formulation of TS theory, $\Delta S^{\ddagger}$ has a significant effect on the computed rate constant of both reactions 8 and 9 ($\Delta S_8^{\ddagger} = 5.8$ cal mol^{-1} K^{-1}, $\Delta S_9^{\ddagger} = -27.6$ cal mol^{-1} K^{-1}), resulting in a computed rate constant for reaction 8 which is greater than that of reaction 9 as is observed. This is despite the fact that the $\Delta H^{\ddagger}$ of reaction 8 is calculated to be more positive than that of reaction 9 ($\Delta H_8^{\ddagger} = 7.5$ kcal mol^{-1}, $\Delta H_9^{\ddagger} = 0.9$ kcal mol^{-1}). For both of these reactions, although temperature changes have effects on $\Delta H^{\ddagger}$ and $\Delta S^{\ddagger}$, and hence on the computed rate coefficient, conventional TS theory cannot account for the effect on the rate coefficient of the presence of the valley, the reactant-like intermediate, before the highest energy point on the reaction surface. Consequently, no attempt was made to compute the temperature dependence of the rate coefficients using conventional TS theory. Nevertheless, from the computed reaction profiles of both reactions 8 and 9, the observed slightly negative temperature dependence of the rate coefficient would imply an anion−molecule intermediate in accordance with expectations based on the results of molecular orbital calculations performed in this work.

Concluding Remarks

The reaction $OH^- + CH_2F_2 \rightarrow$ products has been studied by SIFT experiments and high-level ab initio calculations. The two main reaction channels, reactions 8 and 9, which lead to the anionic products CHF_2^- (86%) and F^- (11%), were computed to be endothermic by 7.5 and exothermic by 20.4 kcal mol^{-1} (ΔH values at 298 K), respectively, at the CCSD-(T)/6-311++$G^{3df,2p}$//MP2/6-31++G** level. The reaction path obtained for reaction 8 at the MP2/6-31++G** level shows that it proceeds with neither a TS nor a product-like intermediate. For reaction 9, however, a TS was located with its structure suggesting a S_N2 mechanism. For both reaction 8 and reaction 9, the initial step is the formation of a reactant-like intermediate. This valley on the reaction path is probably the cause of the observed slight negative temperature dependence of the overall bimolecular rate coefficient.

The product ion yields, which show that $[CHF_2^-] > [F^-]$, are not in accordance with relative magnitudes expected on the basis of the enthalpies for reactions 8 and 9. This difference has been rationalized using the entropy difference between the reagents and the transition state in both reactions ($\Delta S_8^{\ddagger} = +5.8$ cal mol^{-1} K^{-1}, $\Delta S_9^{\ddagger} = -27.6$ cal mol^{-1} K^{-1}) and calculated rate constants for both reactions using conventional TS theory.

It is, however, clear that conventional TS theory[23] is not appropriate to calculate reliable rate coefficients for reactions such as reactions 8 and 9 studied here, as their reaction surfaces are rather complex. More sophisticated theoretical methods based on the canonical variational TS theory[22,24] which considers a large portion of the hypersurface along the reaction path rather than a single point, the TS, will be required to yield results suitable for a more meaningful comparison with experimental rate constants measured at different temperatures. However, these calculations are beyond the scope of the present investigation. Nevertheless, the present study would be a useful starting point for such further investigations.

Comparing the reaction $OH^- + CH_2F_2$ with a previous related study on $O^- + CH_2F_2$[2], the major channel in the case of the OH^- reaction occurs via proton abstraction; this is in accordance with the results of the previous work on $O^- + CH_2F_2$.[2] However, the $OH^- + CH_2F_2$ room temperature rate coefficient is smaller than the $O^- + CH_2F_2$ room temperature rate constant (1.8×10^{-9} cm^3 $molecule^{-1}$ s^{-1})[14] by 3 orders of magnitude,

despite the fact that the PA of OH^- is larger than the PA of O^- by 8.4 kcal mol^{-1}. This is because the reaction rate is determined by the highest part of the reaction hypersurface rather than the portion of the hypersurface associated with the initial steps. Therefore, in the interpretation of the kinetic results, the details of the whole reaction hypersurface are required. Nevertheless, from the present and previous study,[2] it seems that the proton abstraction step is an important initial step in this type of anion−molecule reaction.

The 298 K heats of formation of CHF_2^- and $CH_2(OH)F$ and the electron affinity of CHF_2 were deduced to be −77.8 and −103.0 kcal mol^{-1} and 0.85 eV, respectively.

Acknowledgment. The authors are grateful to CBD (MOD, Porton Down) for financial support and EPSRC for computing resources. Valuable discussions with Dr. A. J. Bell (MOD, Porton Down) are also gratefully acknowledged.

References and Notes

(1) Smith, K. M.; Duxbury, G.; Newnham, D. A.; Ballard, J. *J. Chem. Soc., Faraday Trans.* **1997**, *93*, 2735.

(2) Lee, E. P. F.; Dyke, J. M. *Mol. Phys.* **1996**, *88*, 143.

(3) (a) Grimsrud, E. P. *Mass Spectrom. Rev.* **1992**, *10*, 457. (b) Eiceman, G. A.; Karpas, Z. *Ion Mobility Spectrometry*; CRC Press: Boca Raton, FL, 1994. (c) Harrison, A. G. *Chemical Ionization Mass Spectrometry*; CRC Press: Boca Raton, FL, 1992.

(4) (a) Grabowski, J. J.; Melly, S. J. *Int. J. Mass Spectrom. Ion Processes* **1987**, *81*, 147. (b) Lee, J.; Grabowski, J. J. *Chem. Rev.* **1992**, *92*, 1611.

(5) (a) Ferguson, E. E.; Fehsenfeld, F. C.; Albritton, D. L. *Gas-Phase Ion Chemistry*; Bowers, M. T., Ed.; Academic Press: New York 1979; Vol. 1. (b) Wayne, R. P. *Chemistry of Atmospheres*, 2nd ed.; Clarendon Press: Oxford, 1991. (c) Arnold, F.; Viggiano, A. A.; Ferguson, E. E. *Planet. Space Sci.* **1982**, *30*, 1307.

(6) *CRC Handbook of Chemistry and Physics*, 77th ed.; Editor-in-chief: Lide, D. R., Ed.; CRC Press: Boca Raton, FL, 1996/97.

(7) Smith, D.; Adams, N. G. *Adv. At. Mol. Phys.* **1988**, *24*, 1.

(8) Rodriquez, C. F.; Sirois, S.; Hopkinson, A. C. *J. Org. Chem.* **1992**, *57*, 4869.

(9) Pople, J. A.; Head-Gordon, M.; Fox, D. J.; Raghavarchari, K.; Curtiss, L. A. *J. Chem. Phys.* **1989**, *90*, 5622.

(10) Curtiss, L. A.; Raghavarchari, K.; Pople, J. A. *J. Chem. Phys.* **1993**, *98*, 1293.

(11) (a) Curtiss, L. A.; Raghavarchari, K.; Trucks, G. W.; Pople, J. A. *J. Chem. Phys.* **1991**, *94*, 7221. (b) Curtiss, L. A.; Carpenter, J. E.; Raghavarchari, K.; Pople, J. A. *J. Chem. Phys.* **1992**, *96*, 9030.

(12) Boys, S. F.; Bernardi, F. *Mol. Phys.* **1970**, *19*, 553.

(13) Frish, M. J.; Trucks, G. W.; Schlegel, H. B.; Gill, P. M. W.; Johnson, B. G.; Robb, M. A.; Cheesemans, J. R.; Keith, T. W.; Petersson, G. A.; Montgomery, J. A.; Raghavachari, K.; Al-Laham, M. A.; Zakrzewski, V. G.; Ortiz, J. V.; Foresman, J. B.; Cioslowski, J.; Stefanov, B. B.; Nanayakkara, A.; Challacombe, M.; Peng, C. Y.; Ayala, P. Y.; Chen, W.; Wong, M. W.; Andres, J. L.; Replogle, E. S.; Gomperts, R.; Martin, R. L.; Fox, D. J.; Binkley, J. S.; De Frees, D. J.; Baker, J.; Stewart, J. P.; Head-Gordon, M.; Gonzalez, C.; Pople, J. A. *GAUSSIAN 94*; Gaussian Inc.: Pittsburgh, PA, 1995.

(14) Peverall, R.; Kennedy, R. A.; Mayhew, C. A.; Watts, P. *Int. J. Mass Spectrom. Ion Processes* **1997**, *171*, 51.

(15) For example, Sumath, R.; Peyerimhoff, S. D. *J. Chem. Phys.* **1997**, *107*, 1872.

(16) JANAF Thermodynamical Tables, 2nd ed.; Stull, D. R., Prophet, H., Project Directors; NSRDS−NBS: 1971; Vol. 37.

(17) Pickard, J. M.; Rogers, A. S. *Int. J. Chem. Kinet.* **1983**, *15*, 569.

(18) Luke, B. T.; Loew, G. H.; McLean, A. D. *J. Am. Chem. Soc.* **1987**, *109*, 1307.

(19) McMillen, D. F.; Golden, D. M. *Annu. Rev. Phys. Chem.* **1982**, *33*, 493.

(20) Lias, S. G.; Bartmess, J. E.; Liebman, J. F.; Levine, R. D.; Mallard, W. G. *J. Phys. Chem. Ref. Data* **1988**, *17*, Supplement 1.

(21) (a) Graul, S. J.; Squires, R. R. *J. Am. Chem. Soc.* **1990**, *112*, 2517. (b) Mallard, W. G., Ed. NIST Standard Reference Data Base, 1969−March 1998, from NIST Chemistry WebBook. http://webbook.nist.gov/.

(22) Espinosa-Garcia, J.; Corchado, J. C. *J. Phys. Chem. A* **1997**, *101*, 7336.

(23) $k(T) = k_b T/h \exp(-\Delta G^{\ddagger,T}/RT)$, where $\Delta G^{\ddagger,T} = \Delta H^{\ddagger} - T\Delta S^{\ddagger}$, from Avery, H. E. *Basic Reaction Kinetics and Mechanisms*; MacMillan: London, 1974.

(24) De Turi, V. F.; Hirtz, P. A.; Ervin, K. M. *J. Phys. Chem. A* **1997**, *101*, 5969.